Lab-on-a-Chip Hot Paper

Deutsche Ausgabe: DOI: 10.1002/ange.201503727
Internationale Ausgabe: DOI: 10.1002/anie.201503727

Autonomous Chemical Sensing Interface for Universal Cell Phone Readout**

*Germán Comina, Anke Suska, and Daniel Filippini**

Abstract: *Exploiting the ubiquity of cell phones for quantitative chemical sensing imposes strong demands on interfacing devices. They should be autonomous, disposable, and integrate all necessary calibration and actuation elements. In addition, a single design should couple universally to a variety of cell phones, and operate in their default configuration. Here, we demonstrate such a concept and its implementation as a quantitative glucose meter that integrates finger pumps, unidirectional valves, calibration references, and focusing optics on a disposable device configured for universal video acquisition.*

Currently, cell phones offer a powerful, widespread, and continuously renewed infrastructure, which is compatible with autonomous and decentralized chemical sensing and diagnostics.[1–4] Three main instrumentation alternatives can be distinguished: 1) standalone instruments electrically interfaced to cell phones for processing and communication,[1,5] 2) reusable accessories that exploit optical coupling for readout,[1,2,6,7] and 3) disposable devices conceived to operate on unmodified cell phones.[8,9] These alternatives illustrate the compromise between the freedom to design the instruments and their ubiquity, which is only entirely preserved with disposable devices. Such devices can couple powerful detection principles like surface plasmon resonance detection[8] on regular microfluidic systems;[10] however, the consolidation of this strategy requires totally autonomous and generic systems able to integrate essential functions, such as actuation, sample handling, calibration, chemical transduction, and optical coupling, with a single architecture.

Autonomous lab-on-a-chip (LOC) devices have been investigated by several groups.[11–15] However, suitable concepts for quantitative readouts on unmodified cell phones demand the integration of calibration ranges and robust detection methods, to make them compatible with any phone model, operating system, and user settings.

Here, we present an autonomous disposable system fulfilling all these requirements and introducing an integrated finger pump, that supports repeated pumping actions, an integrated calibration range, and 3D printed optics for universal coupling to cell phone cameras.

[*] Dr. G. Comina, Dr. A. Suska, Prof. Dr. D. Filippini
Optical Devices Laboratory, IFM, Linköping University
58183 Linköping (Sweden)
E-mail: danfi@ifm.liu.se

[**] This work was supported by grants to D.F. from the Swedish Research Council (VR) and the Carl Tryggers Foundation.

Supporting information for this article is available on the WWW under http://dx.doi.org/10.1002/anie.201503727.

The devices can be entirely fabricated with low-cost fast-prototyping 3D printing methods, such as the unibody LOC (ULOC)[16,17] concept, which in this work extends its capabilities to optical components. The concept is demonstrated for a colorimetric glucose assay in the clinically relevant range,[18] where the chemistry was conditioned to replace intensity quantification by response time. In this way, detection was made robust to illuminating conditions, and the resolution improved form a maximum of 255 intensity levels to 33 ms (at regular 30 fps video acquisition), literally with the same phone camera.

Pumps are commonly complementary to LOC devices, whereas integration into disposables demand alternative approaches.[19,20] When the total sample volume is less than the internal volume of the device, lateral flow devices[21] or paper microfluidics[22,23] can be used, although their fabrication involves a different set of tools and architectures from classical LOC. Microfluidic capillary systems[24,25] can also provide passive transport, with similar operational limitations, but use advanced micro fabrication resources.[25]

Finger actuation offers an alternative for generic operation and design. Existing solutions rely on specialized pumping elements,[26] which are typically configured to a fixed volume, support a single pumping action, or demand a large footprint for the pumping element.[11,26–28] The finger pump illustrated in Figure 1 is a compact configuration for manual on-demand pumping using standard silicone tubing and integrated check-valves, which offers unlimited pumping volume and repeated pumping actions.

The complete ULOC prototype costs 1.38 US$/device, including the 3D printed optics. The device (Figure 1) manually commands the preparatory sequence of mixing two reagents and three analyte concentrations with minimal user intervention, limited to finger actuation at a single point. The focusing optics was created with the same 3D printing platform (see Supporting Information (SI) for details and Figure SI1), and was conceived to image the ULOC detection region on different cell phone cameras (Figure SI2).

Once the preparatory sequence has been activated, the device is placed on the front facing camera of the phone and the default application for video acquisition is run for quantitative analysis. After 7 min, the device can be detached and disposed, rendering the phone intact for its regular use.

A universal solution demands a design that can be readable with any cell phone. Such a solution is a device that simply sits on the phone screen and aligns to the front camera, wherever it is placed on the phone model. This configuration implies imaging the detection region at 5 mm from the camera surface, which is outside the focal range for cell phones. Thus, a 3D printed focusing lens was developed

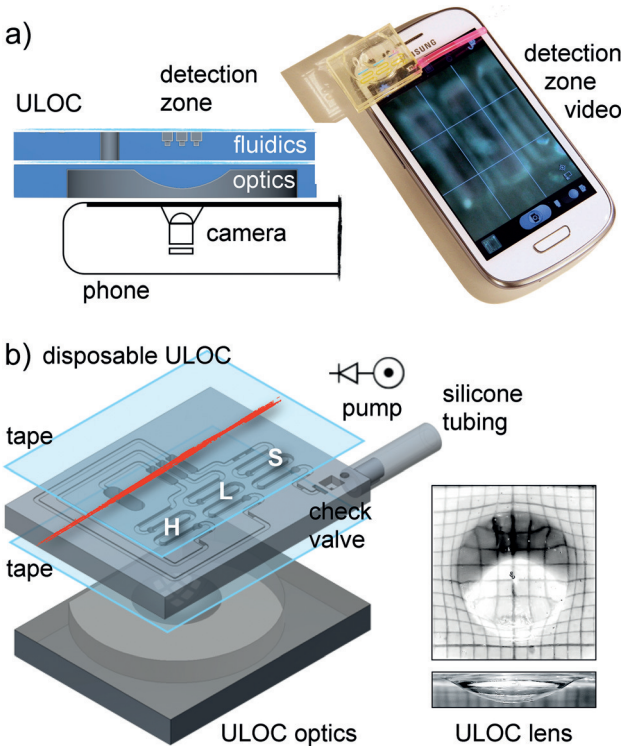

Figure 1. a) Schematics of autonomous LOC device cross-section sitting on a cell phone surface, with detail of the optics and fluidics showing the detection zones and the waste reservoir; actual image of the disposable ULOC device on a Samsung Galaxy S3 Mini cell phone displaying the captured detection zone under ambient illumination. b) 3D scheme of the ULOC device detailing the fluidic component hosting three concentration channels, a check-valve seat, and an integrated connector to silicone tubing. Actual top view of the 3D printed lens on a millimeter paper showing lens magnification and a side view of the lens.

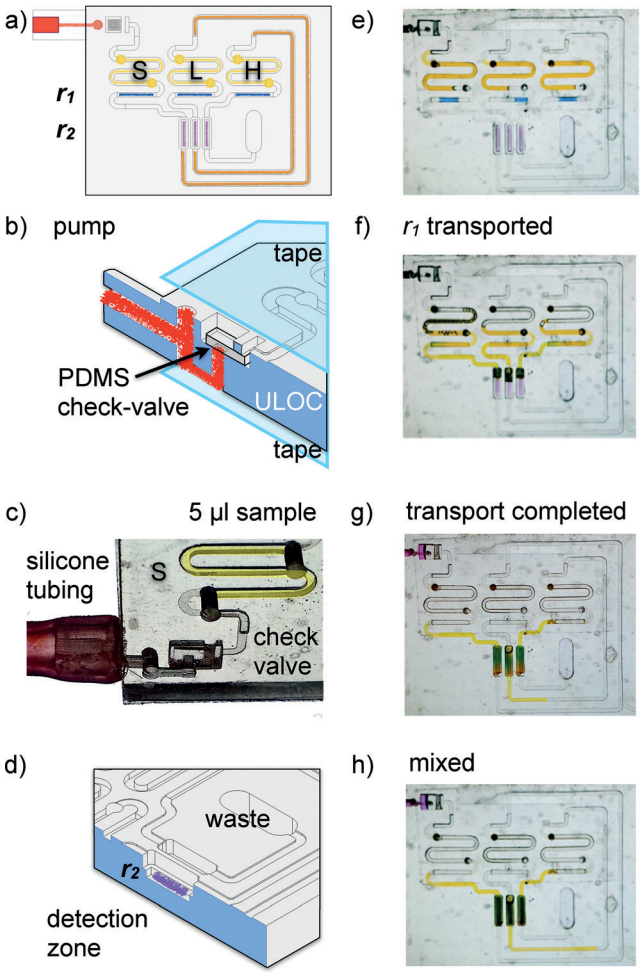

Figure 2. a) Top view of the fluidic layout highlighting in yellow the areas reserved for sample (S, 5 µL), low calibration concentration (L), and high concentration (H). Blue areas correspond to reagent 1 (r_1), magenta detection regions contain reagent 2 (r_2), and brown channels indicate the series connections between zones. b) Schematic 3D cross section of the finger pump showing the 3D printed connector to the silicone tubing and the integrated seat for the check-valve PDMS element, depicting in magenta the pumping fluid. c) Image of the pump and S volume-metering feature through the clear view back side of the device. d) Capture feature for reagent 2 at the bottom of the detection zone. e) Video frame of the device ready for operation. f) Device after pump operation showing complete transport and mixture with reagent 1. g) S, L, and H volumes just delivered in the detection zone. h) S, L, and H volumes at the detection zone once mixed.

for this purpose (Figure 1b and Figures SI1 and SI2 for details).

Although the surface finish delivered by the 3D printer is sufficient for the fluidics, it is not appropriate for optical surfaces. Post-processing for printed lenses was developed that does not require machining, chemical, or mechanical polishing, and achieves a final result that is defined by the printout geometry and allowing for systematic fabrication (see SI for details).

Coherent responses and quantitative results within the calibration range require accurately defined reagent and sample volumes. This is provided by device features that facilitate placing reagents and measuring sample and calibration volumes, which can be delivered with uncalibrated pipettes or syringes (see SI and Figure SI2). Common volume metering features, such as T-junctions,[10] claim significant footprints in classical architectures, whereas the ULOC has space in the unibody bulk for creating specialized features in the vertical direction, with minimal impact on the footprint (Figure 2c).

The ULOC embedded calibration range ensures that the chemistry produces a colorimetric response that can be properly quantified; however, the device utilizes ambient light for illumination, and the calibration range does not eliminate background light variations that can affect the intensity across the field of view. Therefore, the use of intensity for quantitative analysis must be dismissed. Additionally, in the best case, regular phone cameras resolve only 256 levels/channel, whereas a 7 min video acquired at 30 fps can resolve a response peak in 150 s or 4500 data points, which is approximately a 17-fold boost in resolution, using the same camera. To exploit the robustness of time detection, which is immune to spurious background modulations (see Figure SI3 for actual cases), the assay chemistry had to be conditioned to render response peaks proportional to glucose concentration.

The freedom to create 3D features at no extra cost facilitates the configuration of the reagent containers in line

with the channels, which match the pipette tip and capture the reagent volume (0.5 μL) by surface tension, while leaving an open space to prevent displacement by trapped air, until the channels are intentionally flushed.

Classical LOC architectures rely on parallel-branched multiplexers to run simultaneous processes.[10] These branches are simple to equalize, because conventional designs restrict channel depth changes due to cost and added fabrication complexity. Conversely, the ULOC device can incorporate as many 3D features as necessary, but that complicates equalization in parallel configurations. Thus, a series configuration was adopted, which is not only robust to geometric differences but also reduces the footprint. When the unibody is sealed, trapped air acts as a plunger between zones (colored brown in Figure 2a) that simultaneously displaces the carrier fluid (5 μL S, L, and H calibration solutions, colored in yellow in Figure 2a), when externally actuated (Figure 2).

The pumping system consists of a pumping fluid (water) contained in the silicone tubing (colored magenta in Figure 1 and Figure 2). This fluid fills the lumen of the pumping element, which is a 2.5 cm segment of regular silicone tubing (1.5 mm inner diameter). Compressing the free side of the tubing pumps fluid in the check-valve forward direction and displaces the air trapped ahead in the channels (Figure 2b), which propagates along the S, L and H zones.

Unidirectional flow is attained with the integrated check-valve, which prevents backward flow when the tubing is released after each pumping action. This check-valve architecture[29] uses an asymmetric seat geometry to seal a orifice with a rectangular elastic element (Figure 2b) made of a polydimethylsiloxane (PDMS) film. The flow was demonstrated to be unidirectional in the 70 psi (482 kPa) range,[30] far beyond the 75.11 Pa pressure attainable by manual action (see SI for characterization and Figure SI4).

When the pump is actuated, the volume V_S (5 μL, as well as V_L and V_H) is displaced (Figure 2a,c) and acts as a carrier fluid mixing with and transporting Vr_1 (0.5 μL, reagent 1) into the detection zone, where it mixes with Vr_2 (0.5 μL, reagent 2) immobilized in the detection zone (Figure 2d). The glucose test reagent 1 consists of the mixed enzymes glucose oxidase (GOx) and horseradish peroxidase (HRP), while reagent 2 is the HRP substrate, Ampliflu Red (details in SI).

Selected video frames (Figure 2e–h) illustrate the assembled device, with colored solutions, before operation (Figure 2e) showing the substances properly contained in specific regions of the ULOC device. In the first 4 s after pumping (Figure 2 f,g), the reagents are completely mixed and transported to the detection region, which is evident by the total removal of blue dye and the generation of a green mixture.

In the detection zone, the 5.5 μL mixture of sample and reagent 1 are exposed to the entire underside of this region, which hosts reagent 2 (Figure 2 g). After 80 s all components are mixed (Figure 2 h and Figure SI5), and the reactions in the three zones (S, L and H) are progressing for time-lapsed quantification.

In addition to its relevance as the dominant biosensing target,[31] the implemented glucose sensing approach demonstrates a generic configuration applicable to many other sensing targets. Figure 3 shows the evaluation of the actual

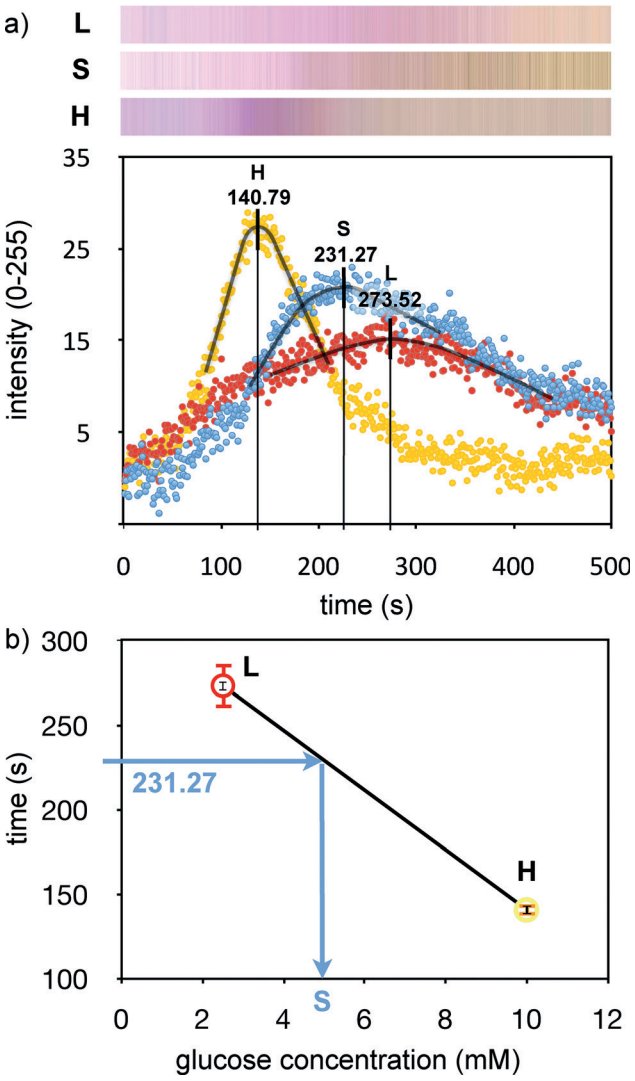

Figure 3. a) Collection of glucose assay responses to L, S, and H concentrations (2.5, 5 and 10 mM, respectively) and the average green channel intensity value of the regions of interest (ROIs), with indicated times corresponding to the maximum color responses. b) Calibration range established by the L and H values and the measured S concentration corresponding to 5 mM of glucose. Black error bars correspond to the optical detection and are magnified 100 times. Color error bars represent the assay variability for sixplicates.

glucose test. It is based on the classical GOx reaction with glucose (in S, L, and H), which produces hydrogen peroxide that reacts with HRP to catalyze the conversion of the colorless substrate Amplifu red into pink resorufin.[32] In the typical configuration, the color intensity is used to quantify the glucose concentration. For reasons already discussed, the chemistry was conditioned to produce a distinctive time response. Because resorufin is also a substrate for HRP, pink resorufin also vanishes over time proportionally to the glucose concentration. Thus, reagents were adjusted to observe the color decay for the complete concentrations range (L, H).

Figure 3a illustrates the collection of the color response from the ROIs defined on the captured image of the LOC detection zone. The average intensity of the ROI pixels in the

green channel was computed to compose the time response (Figure 3a and SI for details, only 1 fps is shown for clarity). As noted for the actual situation, the complete intensity range is less than 35 intensity levels, but since the intensity is only used to register the peak time, the system can still operate at 33 ms resolution despite of noise, as well as temporal and spatial variations of the illumination. At the current prototype stage the assay contributes variability between devices of $\Delta L = \pm 5.10\,\%$ and $\Delta H = \pm 2.58\,\%$, respectively (Figure SI6).

Most recent phones are equipped with slow motion recording at 120 and 240 fps, equivalent to a 4- and 8-fold boost in resolution, respectively. Alternatively, operating at the present resolution such frame rates would allow 4- and 8-fold faster assay configurations. This would require a more advanced mixing stage, which should also minimize variability.

Determining the peak time for the L and H values (273.52 ± 0.033 s and 140.79 ± 0.033 s, respectively), a calibration range can be constructed (Figure 3b). Thus, for the S value of 231.27 ± 0.033 s the quantified concentration is 5.061 mM, equivalent to an error of 1.22 % with respect to the used glucose concentration of 5 mM.

These results illustrate the autonomous quantitative detection of a chemical parameter, whereas its extension to end-to-end biomedical uses should integrate blood extraction and separation stages,[33] as well as the migration of these prototypes to scalable manufacturing and medical grade materials.

This work demonstrated a sensible combination of technologies to enable practical autonomous LOC sensing on cell phones. This particular solution is conceived to serve any cell phone with a single disposable LOC design, which preserves the ubiquity of the phone. The possibility to operate on cell phones of diverse brand, model, operating system, and acquisition software, makes the interfacing solution universal.

The demonstrated concept performs a generic set of sample conditioning procedures, which were demonstrated for glucose detection and are representative of numerous detection targets.

The concept intrinsically targets universal acquisition using default video applications available in cell phones, which constitutes a standardized output format and a familiar interface for potential users. To exploit these advantages with an autonomous device that utilizes ambient light for illumination, the detection strategy was refined to be robust to background intensity modulations, and optimized to exploit the imaging resources, thereby providing enhanced resolution with the same instrument.

Keywords: 3D printed fluidics · analytical methods · autonomous lab-on-a-chip · cell phone readout · sensors

How to cite: *Angew. Chem. Int. Ed.* **2015**, *54*, 8708–8712
Angew. Chem. **2015**, *127*, 8832–8836

[1] a) S. Kumar-Vashist, O. Mudanyali, E. M. Schneider, R. Zengerle, A. Ozcan, *Anal. Bioanal. Chem.* **2014**, *406*, 3263–3277; b) T. Laksanasopin, T. W. Guo, Sa. Nayak, A. A. Sridhara, S. Xie, O. O. Olowookere, P. Cadinu, F. Meng, N. H. Chee, J. Kim, C. D. Chin, E. Munyazesa, P. Mugwaneza, A. J. Rai, V. Mugisha, A. R. Castro, D. Steinmiller, V. Linder, J. E. Justman, S. Nsanzimana, S. K. Sia, *Sci. Trans. Med.* **2015**, *7*, 273re1; c) M. D'Ambrosio, M. Bakalar, S. Bennuru, C. Reber, A. Skandarajah, L. Nilsson, N. Switz, J. Kamgno, S. Pion, M. Boussinesq, T. B. Nutman, D. A. Fletcher, *Sci. Trans. Med.* **2015**, *7*, 286re4.

[2] P. Preechaburana, A. Suska, D. Filippini, *Trends Biotechnol.* **2014**, *32*, 351–355.

[3] A. Nemiroski, D. C. Christodouleas, J. W. Hennek, A. A. Kumar, E. J. Maxwell, M. T. Fernández-Abedul, G. M. Whitesides, *Proc. Natl. Acad. Sci. USA* **2014**, *111*, 11984–11989.

[4] R. Potyrailo in *Springer Series on Chemical Sensors and Biosensors*, *Vol. 13* (Series Ed.: G. Urban), Springer, Heidelberg, Berlin, **2013**, Chap. 10, pp. 237–264.

[5] P. Preechaburana, A. Suska, D. Filippini in *Mobile Point-of-Care Monitors and Diagnostic Device Design* (Eds.: K. Iniewsky, W. Karlen), CRC, Boca Raton, **2015**, Chap. 1, pp. 3–22.

[6] A. F. Coskun, H. Zhu, O. Mudanyali, A. Ozcan in *Mobile Point-of-Care Monitors and Diagnostic Device Design* (Eds.: K. Iniewsky, W. Karlen), CRC, Boca Raton, **2015**, Chap. 2, pp. 21–40.

[7] Q. Wei, W. Luo, S. Chiang, T. Kappel, C. Mejia, D. Tseng, R. Y. L. Chan, E. Yan, H. Qi, F. Shabbir, H. Ozkan, S. Feng, A. Ozcan, *ACS Nano* **2014**, *8*, 12725–12733.

[8] P. Preechaburana, M. Collado Gonzalez, A. Suska, D. Filippini, *Angew. Chem. Int. Ed.* **2012**, *51*, 11585–11588; *Angew. Chem.* **2012**, *124*, 11753–11756.

[9] P. Preechaburana, A. Suska, D. Filippini, *Sensors* **2012**, *12*, 8586–8600.

[10] *Microfluidics and Nanofluidics Handbook, Fabrication, Implementation, and Applications* (Eds.: S. Mitra, S. Chakraborty), CRC, Taylor & Francis, Boca Raton, **2012**.

[11] T. Kokalj, Y. Park, M. Vencelj, M. Jenko, L. P. Lee, *Lab Chip* **2014**, *14*, 4329–4333.

[12] L. Qin, O. Vermesh, Q. Shi, J. R. Heath, *Lab Chip* **2009**, *9*, 2016–2020.

[13] R. Bharadwaj, A. Singh in *Springer Series on Chemical Sensors and Biosensors, Vol 13* (Series Ed.: G. Urban), Springer, Heidelberg, Berlin, **2013**, Chap. 9, pp. 217–236.

[14] D. Mabey, R. W. Peeling, A. Ustianowski, M. D. Perkins, *Nat. Rev. Microbiol.* **2004**, *2*, 231–240.

[15] M. Urdea, L. A. Penny, S. S. Olmsted, M. Y. Giovanni, P. Kaspar, A. Shepherd, P. Wilson, C. A. Dahl, S. Buchsbaum, G. Moeller, D. C. Hay Burgess, *Nature* **2006**, *444*, 73–79.

[16] G. Comina, A. Suska, D. Filippini, *Lab Chip* **2014**, *14*, 2978–2982.

[17] G. Comina, A. Suska, D. Filippini, *Lab Chip* **2014**, *14*, 424–430.

[18] S. F. Clarke, J. R. Foster, *Br. J. Biomed. Sci.* **2012**, *69*, 83–93.

[19] V. Gubala, L. F. Harris, A. J. Ricco, M. X. Tan, D. E. Williams, *Anal. Chem.* **2012**, *84*, 487–515.

[20] A. Nisar, N. Afzulpurkar, B. Mahaisavariya, A. Tuantranont, *Sens. Actuators B* **2008**, *130*, 917–942.

[21] G. A. Posthuma-Trumpie, J. Korf, A. van Amerongen, *Anal. Bioanal. Chem.* **2009**, *393*, 569–582.

[22] a) W. M. Martinez, S. T. Phillips, B. J. Wiley, M. Guptaa, G. M. Whitesides, *Lab Chip* **2008**, *8*, 2146–2150; b) W. M. Martinez, S. T. Phillips, G. M. Whitesides, *Anal. Chem.* **2010**, *82*, 3–10.

[23] J. L. Osborn, B. Lutz, E. Fu, P. Kauffman, D. Y. Stevens, P. Yager, *Lab Chip* **2010**, *10*, 2659–2665.

[24] D. Juncker, H. Schmid, U. Drechsler, H. Wolf, M. Wolf, B. Michel, N. de Rooij, E. Delamarche, *Anal. Chem.* **2002**, *74*, 6139–6144.

[25] a) M. Zimmermann, H. Schmid, P. Hunziker, E. Delamarche, *Lab Chip* **2007**, *7*, 119–125; b) L. Gervais, E. Delamarche, *Lab Chip* **2009**, *9*, 3330–3337.

[26] S. Begolo, D. V. Zhukov, D. A. Selck, L. Li, R. F. Ismagilov, *Lab Chip* **2014**, *14*, 4616–4628.

[27] a) W. Yang, Y. G. Nam, B. K. Lee, K. Han, T. H. Kwon, D. S. Kim, *Jpn. J. Appl. Phys.* **2010**, *49*, 06M01; b) X. Qiu, J. A. Thompson, Z. Chen, C. Liu, D. Chen, S. Ramprasad, M. G. Mauk, S. Ongagna, C. Barber, W. R. Abrams, D. Malamud, P. L. A. M. Corstjens, H. H. Bau, *Biomed. Microdevices* **2009**, *11*, 1175 – 1186; c) V. F. Curto, S. Coyle, R. Byrne, N. Angelov, D. Diamond, F. Benito-Lopez, *Sens. Actuators B* **2012**, *175*, 263 – 270.
[28] K. Iwai, K. C. Shih, X. Lin, T. A. Brubaker, R. D. Sochol, L. Lin, *Lab Chip* **2014**, *14*, 3790 – 3799.
[29] B. Yang, Q. Lin, *Sens. Actuators A* **2007**, *134*, 186 – 193.
[30] G. Comina, A. Suska, D. Filippini, *Micromachines* **2015**, 5, 437 – 451.
[31] A. P. F. Turner, *Chem. Soc. Rev.* **2013**, *42*, 3184 – 3196.
[32] a) V. Towne, M. Will, B. Oswald, Q. Zhao, *Anal. Biochem.* **2004**, *334*, 290 – 296; b) M. Zhou, Z. Diwu, N. Panchuk-Voloshina, R. P. Haugland, *Anal. Biochem.* **1997**, *253*, 162 – 168.
[33] a) C. Li, M. Dangol, C. Y. Lee, M. Jang, H. Jung, *Lab Chip* **2015**, *15*, 382 – 390; b) I. Dimov, L. Basabe-Desmonts, J. L. Garcia-Cordero, B. M. Ross, A. J. Riccoa, L. P. Lee, *Lab Chip* **2011**, *11*, 845 – 850.

Received: April 23, 2015
Revised: May 21, 2015
Published online: June 10, 2015

